

Towards an Integrated Solution for Renewable Water and Energy

Rex Hung-Gang Chen¹ and Chi-Ming Chen²

¹University Transition Program, University of British Columbia, Vancouver, Canada

²Physics Department, National Taiwan Normal University, Taipei, Taiwan

Summary

In order to provide an integrated solution for two sustainability issues, supplying clean water and using renewable energy sources, we propose a solar desalination plant that uses solar energy for seawater desalination and generating electricity. To test the efficiency of the hypothetical plant, we conducted two small-scale simulations. The first simulation tested our solar tracking robot and how it could maximize the amount of solar energy collected. When the sun's position is near the zenith, our data on the solar azimuth and elevation angles were consistent with theoretical predictions, but the data deviate from theoretical values at other times due to atmospheric refraction, which was not considered in the theory. The second simulation investigated the desalination process by controlling the salinity and surface area, while keeping the water temperature below the boiling point. We found that the volume of water vapor exponentially decreased with salinity and linearly increased with the surface area of the saline water. From our experimental data, we estimated that, by collecting vapor from saline water at a temperature slightly less than the boiling point, the yield of desalinated water was 67% greater than that of the direct evaporation method. Locations where the system would be most efficient are coastal areas between 40 °N and 40 °S, where the ratio between solar radiation and ground water recharge rate is at a maximum.

Received: August 21, 2014; **Accepted:** December 8, 2014; **Published:** January 9, 2015

Copyright: (C) 2015 Chen and Chen. All JEI articles are distributed under the attribution non-commercial, no derivative license (<http://creativecommons.org/licenses/by-nc-nd/3.0/>). This means that anyone is free to share, copy and distribute an unaltered article for non-commercial purposes provided the original author and source is credited.

Introduction

There are three primary urgent sustainability issues that are faced by humanity today: the supply of clean water, the sources of renewable energy, and the treatment of waste material. These issues are relevant on a global scale, and are pressingly urgent, directing an increasing amount of attention and resources to sustainability research.

Situations such as the 2011 East African drought (1), which caused approximately 260,000 casualties in addition to large-scale food refugee crises, and the 2005 Amazonian mass drought (2), which had irreversible effects on the local ecological and climactic systems,

are becoming increasingly prevalent. Such phenomena are heavily influenced by anthropogenic global warming and occur especially in the arid and decertified regions of the Saharan Sahel region and the Australian Outback. Climate change could potentially have more severe implications in the near future. Dai demonstrated using the SRES A1B medium emissions scenario that the Palmer Drought Severity Index (PDSI), or the measure of local dryness based on precipitation and temperature, of regions such as the Mediterranean, Central America, and northern Africa could reach -20 by 2060, nearly fourfold the current lowest value of approximately -5 (3).

Gases such as carbon dioxide, methane, nitrous oxide, and ozone are naturally found in the earth's atmosphere and help to trap solar energy. They contribute to the overall temperature of the earth and maintain the habitable biosphere of the planet. However, anthropogenic greenhouse gases are having

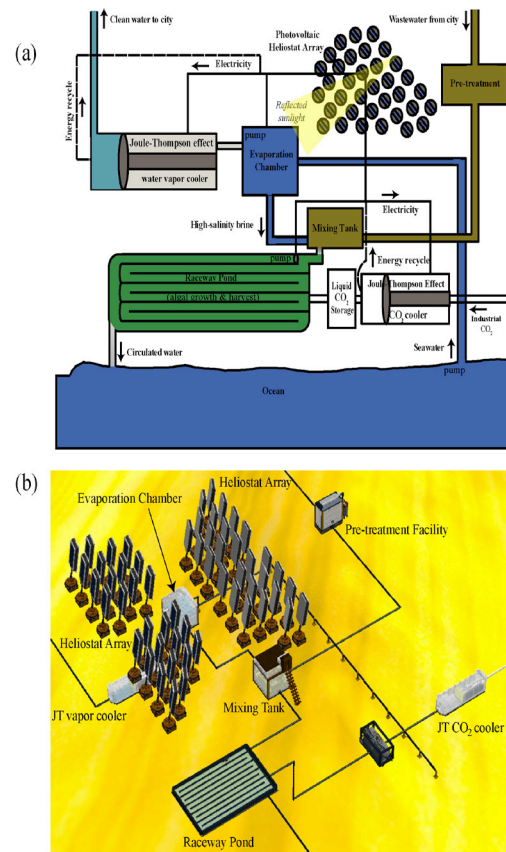


Figure 1: Blueprint (a) and prototypical model (b) of the proposed sustainable desalination plant. The model in (b) is a virtual realization of (a) constructed using the Lego Digital Designer modelling software.

an increasingly drastic impact on the global biosphere. Since the Industrial Revolution, demand for fossil fuels has increased exponentially, and supplies are diminishing rapidly. The burning of fossil fuels releases various greenhouse gases that add to the pre-existing amount, significantly raising the temperature through the greenhouse effect. According to data from the Carbon Dioxide Information Analysis Center, levels of atmospheric methane have increased nearly twofold since 1750 and carbon dioxide has increased by 40%, both due to the emissions of human industrial activities as well as from natural causes (4). Deforestation has also contributed to the rise in atmospheric CO₂ (5). If this trend continues, then the climactic conditions projected by SRES A1B could very easily become reality.

Increased urban and industrial activity after the Industrial Revolution also accompanied a significant output of wastewater. Industrial and municipal wastewater has sometimes been found to contain toxic waste, pesticides, oils, pathogens, human waste, and extreme pH (6). In overcrowded developing areas, such as the Indian peninsula and eastern China, where the quality of sanitation does not fulfill municipal needs, wastewater could easily be recirculated into the urban drinking water system. High precipitation levels in India contribute to the unsanitary conditions by overflowing sewers (7).

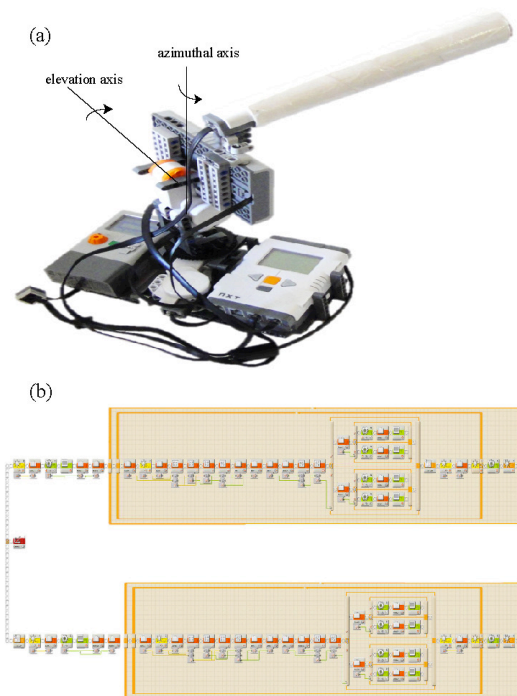


Figure 2. Solar tracking robot (a) and the tracking algorithm (b). The top row of the program controls azimuth while the bottom row controls elevation. In the program, the yellow measurement blocks prompt the robot to measure the ambient luminosity as measured by the light sensor, the orange blocks instruct the robot to perform calculations based on the difference between the luminosity before and after the rotation, and the green blocks control the rotation of the motors.

Industrial pollutants in China are contaminating the drinking water to such an extent that the water cannot be fully purified in any way. In certain areas, pollutants contain a large variety of carcinogens and pathogens that infect inhabitants of entire villages through transmission and bioaccumulation (8).

Thus, a source for clean drinking water powered by renewable energy is highly desirable for regions that are impacted by the adverse effects of the environmental phenomena described above. In order to mitigate the problematic consequences of such phenomena, we proposed a prototypical model for an integrated solution of clean water and renewable energy. The core component of this model is a desalination system that converts seawater to clean drinking water solely through the use of solar energy that is collected from a photovoltaic heliostat array. Each heliostat in the array is a mirror that rotates to keep reflecting sunlight toward a fixed target, regardless of the sun's movement in the sky. We have designed and conducted a series of experiments in order to maximize the efficiency of various components of our model.

Our proposed model, as illustrated in Figure 1, consists primarily of two modules: a seawater transportation and desalination system (the desalination module) and a photovoltaic heliostat array (the energy module). Figure 1a shows the blueprint of our model, and Figure 1b is a virtual prototype of the blueprint that was constructed using the Lego Digital Designer modelling software. In Figure 1b, two heliostat arrays are placed on the east and west sides of the evaporation chamber such that the chamber can receive reflected sunlight throughout the entire day. The Joule-Thompson (JT) cooler for the resulting water vapor, a cooler which liquefies vapor by forcing it through a porous plug while the system is adiabatically isolated (i.e., no heat is exchanged with the environment), is built underground to lower the temperature of the vapor. We note that Figure 1 also includes a separate facility (the waste treatment module) to treat brine, city wastewater, and industrial CO₂ by cultivating algae in a raceway pond; however, simulating the waste treatment module is beyond the scope of this research project.

In the desalination module, seawater is pumped from the ocean, and pre-heated during its transportation by a metal parabolic trough (9). The trough is coated with mirrors that reflect the heat of the sunlight into the transported seawater, which then enters a vaporization chamber. In the chamber, seawater is further heated by the reflected sunlight from the heliostat array, and the generated water vapor can then be pumped into a JT cooler to generate liquid water. The clean liquid water produced by the JT cooler can then be distributed for municipal consumption.

The photovoltaic heliostat array in the energy module is composed of a collection of heliostats that have solar panels on one side and mirrors on the other. The array of heliostats farther away from the sun reflects sunlight into the vaporization chamber with mirrors, while the other half of the array generates electricity with solar panels to

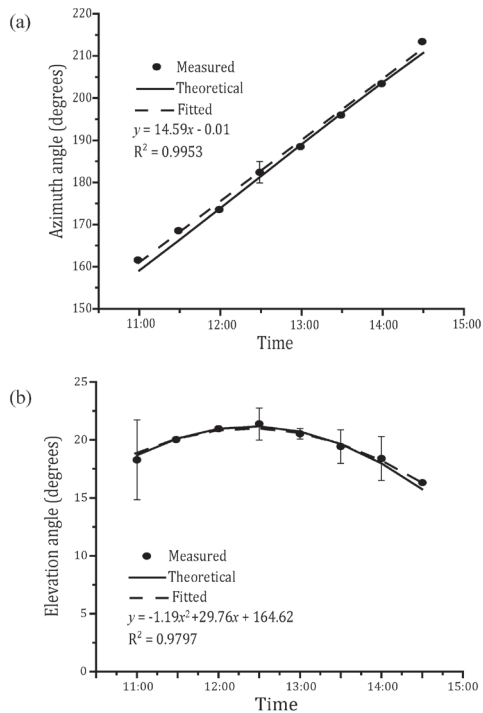


Figure 3: Azimuthal angle vs. time (a) and elevation angle vs. time (b). The graphs reflect the movement of the sun relative to the observer on earth. For the fitted curves in both figures, the x-axis is the time of day, in hours.

power the plant. To prevent energy loss, we propose a desalination process of seawater using collected sunlight instead of the electricity used in conventional systems. The alignment of the photovoltaic heliostat array and the parabolic trough is controlled by an intelligent tracking robot to optimize the performance of the energy module. The recycled heat energy from the JT cooler can also serve as an additional source of energy (10).

To investigate the feasibility of our proposed model and to optimize its efficiency, several central topics require investigation: (I) What is the trajectory and cumulative radiation energy of the sun for an observer on earth over the course of a single day? (II) What is the most efficient desalination method that can be accomplished using the collected solar energy, and what is the efficiency? To answer these questions using commonly available materials, we conducted two small-scale experiments to simulate real-life scenarios. In the first simulation experiment, we constructed a solar tracking robot, which was used to track the position of the sun and generate electricity from collected solar energy. In the second simulation experiment, we desalinated saline water by two methods, direct exposure to the sun and heating with an induction cooker, and used the experimental data to estimate the efficiency of various desalination methods.

Results

In the first simulation that we conducted, we built a solar tracking robot using Lego components and programmed

a tracking algorithm for the robot using the Lego Mindstorms NXT programming language (Figure 2). The tracking device was used to measure the azimuth angle, or the angle of the sun relative to the north, and elevation angle, or the angle of the sun in the sky relative to the horizon, of the sun, such that the collected solar energy could be maximized. Figure 3 compares theoretical values calculated by the SunEarthTools algorithm from planetary orbits (11, 12) and experimental values of the azimuth angle (a) and elevation angle (b) of the sun as measured at University Hill, Vancouver, Canada between 11:00 A.M. and 2:30 P.M. on January 22, 2014. The data from the solar tracking experiment consists of the average azimuthal and elevation angles during the first minute of each half-hour and the standard deviation for each data point (Figure 3). Our data was consistent with theoretical values, with the difference in azimuth being $< \pm 3^\circ$ and the difference in elevation being $\leq \pm 0.6^\circ$.

Figure 4 shows the generated power of the solar panel attached to the tracking device between 9:45 A.M. and 2:45 P.M. on September 4, 2014. The data displayed shows the average amount of solar energy during the first minute of each consecutive 15-minute interval. No data was recorded after 3 P.M., as the sun became obstructed by surrounding buildings. During the trial, the solar panel, with an area of $6 \times 10 \text{ cm}^2$, was able to generate 0.3-0.4 W of power; periods of cloud cover may have halved the generated power and lead to larger fluctuations in it. For calibrating the solar panel's efficiency, we note that the solar panel generates 0.02 W of power when it is under direct light from a 60 W incandescent light bulb positioned 0.25 m from the panel. The yield of our solar panel was estimated to be greater than 4.3%.

The second simulation investigated various desalination methods, and examined how salinity and surface area of saline water affect its evaporation. The simulation was conducted with a small-scale replica, and we utilized the collected data to estimate the yield of our

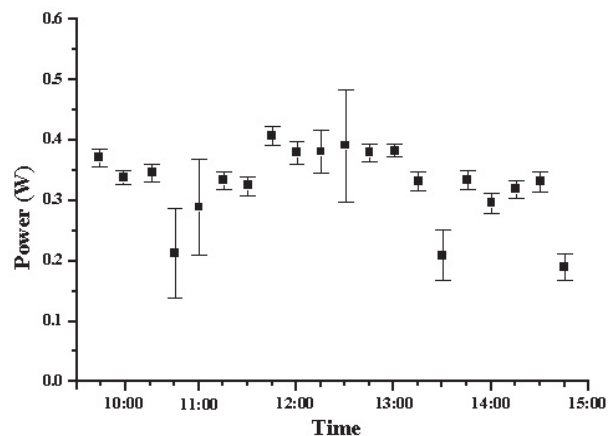


Figure 4: Power generated by a solar panel mounted on the solar tracking robot from 9:45 A.M. to 3:00 P.M. Larger fluctuations in the measured data were caused by cloud cover. Each data point is the average value of measurements from 300 trials. The error bars shown represent the standard deviation of the data.

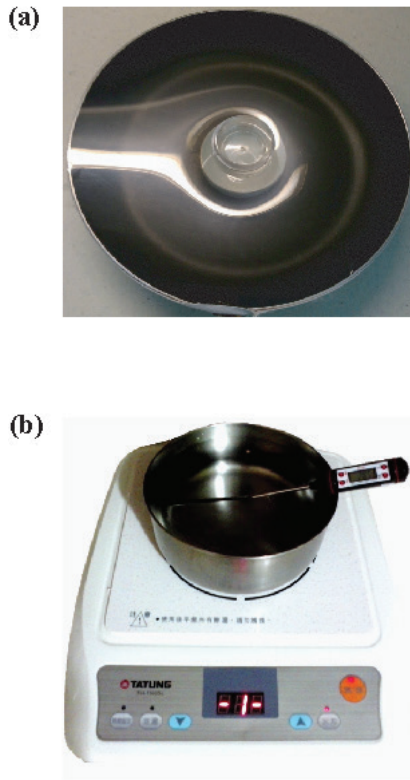


Figure 5: Experimental setup for the simulation of desalination by direct exposure to the sun (a) and by heating with an induction cooker (b). A thermometer was used to monitor water temperature.

novel desalination method, which functions by collecting water vapor at temperatures lower than the boiling point. In this experiment, we first desalinated 1.0 L of saline water, using a pan with a surface area 0.1 m^2 that was under direct exposure to the sun from 10 A.M. to 5 P.M. on September 10, 2014. For the pan without a cover, the amount of evaporated water was measured to be 0.20 L, and the temperature of the saline water varied between $14.2 \text{ }^\circ\text{C}$ and $35.5 \text{ }^\circ\text{C}$. For the pan covered with a plastic wrap, the amount of collected fresh water was 0.06 L (Figure 5a). For comparison, the amount of evaporated water was approximately 0.01 L in a desalination trial without exposure to the sun.

Furthermore, we desalinated 0.6 L of saline water by heating it with an induction cooker (Figure 5b). In Figure 6, we display the measured volume of water vapor during the vaporization process for various salinities and surface areas of saline water. For the same amount of input energy (240 kJ), we found that the amount of water vapor decreases exponentially with salinity and increases linearly with surface area. The fitted curve is $y = 5.41 + 3.14e^{-x/2.27}$ ($R^2=0.9898$) for salinity (Figure 6a) and $y = 0.008z + 4.54$ ($R^2=0.9996$) for surface area (Figure 6b). Here y represents the percentage of water evaporated, x represents the salinity of the solution, and z is the surface area in cm^2 .

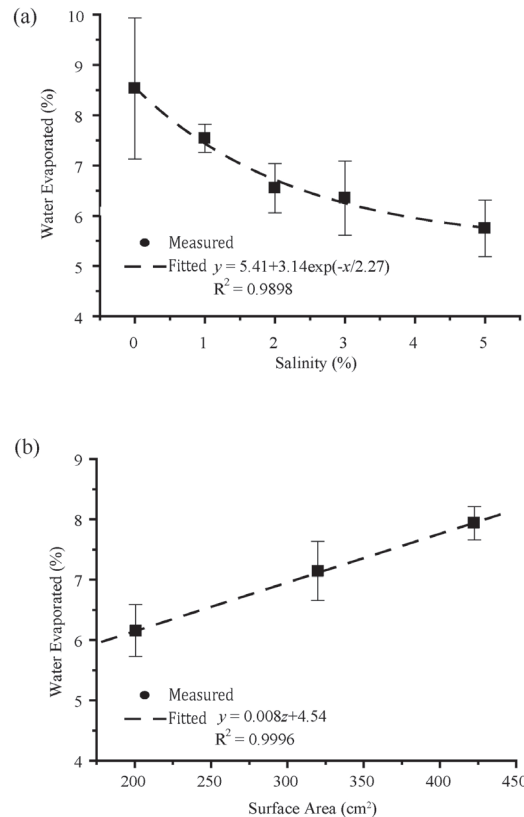


Figure 6: Graphs of water evaporated vs. salinity (a) and water evaporated vs. surface area (b). Note that the volume of evaporated water decays exponentially with salinity, and increases linearly with surface area. Each data point is the average value of measurements from three trials. The error bars shown represent the standard deviation of the data..

Discussion

In the solar tracking experiment, our data on the measured azimuth and elevation angles of the sun are consistent with the theoretical predictions (11, 12) when the sun is near the zenith, or the point on the celestial sphere that is directly above the observer on the vertical axis. However, for positions that are farther away from the zenith, our data may be more accurate than theoretical values, since atmospheric refraction of sunlight is not considered in the theory.

The fluctuations that were observed in the data are mainly due to cloud cover, during which the brightest spot in the sky varied with time, according to the tracking robot. To reduce fluctuation, a cardboard tube was placed over the light sensor in order to allow the robot to focus on a smaller region of the sky, thus increasing the stability of the tracking mechanism. It can be seen that the curves (azimuth angles vs. time and elevation angles vs. time) in Figure 3 are consistent with the general movement of the sun relative to the observer, as the azimuthal angle of the sun increases linearly over the course of a single day, and the elevation angle rises to a peak at mid-day (12:30 pm) then falls, in the form of a typical parabolic

curve. Overall, the results of this experiment show that the logic of this solar tracking program is suitable for use in our prototypical model to maximize the efficiency of energy generation.

Our solar panel had an area of 60 cm² and an efficiency of 4.3%, and it was able to generate a constant power of 0.3-0.4 W under exposure to sunlight. The daytime solar radiation power in Vancouver during early September was estimated to be approximately 1 kW/m², and the average length of a day in Vancouver during September is approximately 12.5 hours. According to the collected data, if our energy module consists of 2000 heliostats of area 100 m² and the solar panels have an efficiency of 15%, it will be able to collect 10⁶ kWh of heat energy and 1.5×10⁵ kWh electrical energy on a cloudless day in the month of September. We note that we have utilized our solar tracking robot to maximize the solar radiation power received by the solar panel in our experiment. However, due to a limited budget in constructing experimental equipment, we could not demonstrate the performance of our solar tracking facility by performing a control for the experiment, i.e., a parallel experiment to measure the generated power of the solar panel without solar tracking. Such a comparison would help us estimate the efficiency of our solar tracking robot and design a more efficient solar tracking algorithm.

To further couple the energy and desalination modules, we conducted an experiment in which 1 L of saline water was desalinated by direct exposure to the sun. After 7 hours of exposure, the amount of evaporated water was found to be 0.20 L, and the highest water temperature measured was 35.5 °C. If the system is simply scaled up, the above mentioned energy module would only be able to produce 2.9×10⁵ L of fresh water. However, it was noted that the vapor pressure of saline water drastically increases with water temperature, as shown in Figure 7. The efficiency of the desalination process would be much higher if the experiment was conducted at a higher water temperature. Since the resources to construct the proposed photovoltaic heliostat array were not available, we attempted to improve the desalination method by simulating the energy module with an induction cooker. Our experimental data were then used to evaluate the feasibility of our proposed desalination plant in regions suffering from severe drought.

The results of the desalination simulation experiment can be used to estimate the efficiency of our proposed desalination method, which was to collect vapor from saline water that was kept at a temperature slightly lower than its boiling point. For direct vaporization, the energy required to vaporize 0.6 L of 15 °C seawater is 1.57×10⁶ J, which can be calculated by the formula $E = ms\Delta T + me_g$, where the former is the energy required to raise the temperature of water and the latter is the energy required to vaporize the water. Here, m is the mass of water, $s=4181$ J/(kgK) is the specific heat, ΔT is the change in temperature, and $e_g = 2260$ kJ/kg is the latent heat of water. The amount of energy that was used to heat the saline water in the simulation is given by the

equation $E = ms\Delta T$. As 600 mL of water was heated from 15 °C to 100 °C in the experiment, the energy required can be calculated to be 2.13×10⁵ J. The ratio between the energy for heating and the energy for complete vaporization was 13.5%, where the average ratio of collected vapor was approximately 6% for saline water of salinity 3.5% in the experiment.

Maintaining the temperature of water slightly below its boiling point may produce more consumable fresh water than simply vaporizing water. To estimate the amount of collected vapor when the saline water is heated, as shown in Figure 7, we fitted standard data of saline water vapor pressure for various temperatures (13) with a polynomial function: $y = s(0.0002x^3 - 0.0175x^2 + 0.7928x - 9.2751)$. In the equation, x is the temperature of saline water, y is the vapor pressure, and s is the molar fraction of water. According to Raoult's Law, the vapor pressure of a solution of a non-volatile solute is equal to the vapor pressure of the pure solvent at the same temperature, multiplied by its mole fraction (0.98 for saline water of salinity 3.5%). Using integration, the amount of collected vapor from heating 15 °C saline water to 100 °C at a constant rate was found to be proportional to the area $A_1 = 2228$ kPa°C under this vapor pressure curve. If the temperature of saline water is kept at slightly below the boiling point (by adding cold saline water and recovering heat loss during vaporization), the amount of water vapor collected is proportional to the area A_2 , which is approximately 8440 kPa°C. In this case, the amount of water vapor collected can be enhanced by a factor of $A_2/A_1 = 3.79$. Therefore, the collected vapor would be 22.7% of the total amount of saline water if the temperature of the water is slightly lower than the boiling point. Therefore, using our proposed desalination method, we can purify 22.7% of the water by using 13.5% of the energy, compared to the direct vaporization method. The yield of desalinated water can be improved by approximately 67%.

We note that, in the above estimation for the

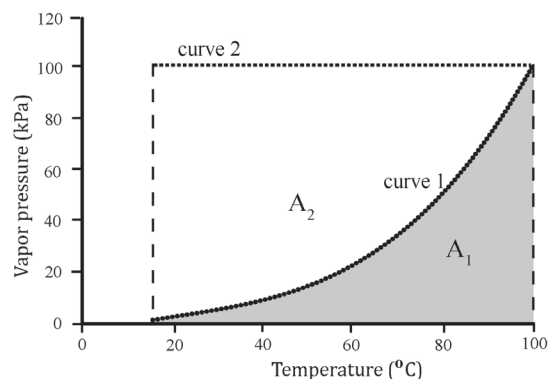


Figure 7: Graph comparing the vapor pressure of two different desalination methods, gradually heating the water up to 100°C (curve 1) and maintaining water temperature slightly below 100°C (curve 2). The volumes of collected water vapor for the methods of desalination are respectively proportional to the area under the curves, A_1 and A_2 .

available amount of fresh drinking water, we measured the amount of evaporated water in our experiments. This estimation assumed that water vapor can be pumped into a cooler to produce fresh drinking water. Such a cooling facility is currently not available in our experiments, but its effects can be simulated using a simple experiment. We covered the pan with a plastic wrap to condensate water vapor and collect fresh drinking water. The yield of this method is approximately 30% of that of a proper cooling facility, as proposed in our model. Such a low yield was expected, as there is no net evaporation of water when the saturation vapor pressure of water is reached in a sealed container. Further evaporation of bulk water in the pan can only occur when the water vapor condenses on the plastic wrap, or when the water temperature increases, which leads to an increase in the saturation vapor pressure. Therefore, it would be more efficient to create fresh drinking water by constantly pumping water vapor into a cooler, which was simulated in our experiments using an open container.

This desalination system was found to have maximum efficiency and desirability in areas between 40°N and 40°S, where the average solar radiation is the highest (14, 15) and the groundwater recharge rate is the lowest (16, 17). In regions suffering from severe drought, the population that can be sustained by the produced water over the course of a day can be calculated using average water consumption data. Using California as a hypothetical scenario, the average solar irradiance in California is approximately 5.4 kWh/m² per day. As previously stated, one half of the photovoltaic heliostat array heats the evaporation chamber, while the other half generates electricity. If each photovoltaic heliostat has a surface area of 100 m², and 1000 mirrors are used to collect heat, the total energy that is collected for heating water is 1.94×10^{12} J per day. Using our proposed desalination method, the desalination plant will produce 1.24×10^6 L water per day. In California, the average domestic water consumption per capita is 47.99 L/day (18), one of the highest rates of water consumption in the United States. This would indicate that our proposed desalination plant is capable of sustaining 25,005 people, which is roughly the size of a small city. However, the city of Los Angeles has a population of 3,884,307 (19), and the entirety of California has a population of 38,322,521 (20). This would mean that 1532 plants would be required to supply enough water for the entirety of California, which has both a large population and a high water consumption rate.

There are other issues and possible applications that are associated with our hypothetical desalination mechanism. We proposed JT coolers as a means of cooling heated vapor by its adiabatic expansion. The work that is done by the JT cooler can be recycled to generate electricity, which may be used to provide additional power to the plant, or be distributed to municipal areas. Efficient mechanisms for recycling the released energy during gas expansion as well as liquefying gas are an area of potential further exploration.

Another area of further study pertaining to this system is the development of an efficient protocol for algae cultivation. This includes the study of the genera of algae that can be used for wastewater treatment in a raceway pond, as well as their applications in biomass, food, and cosmetics. In the waste treatment module, the brine produced during desalination can be mixed with city wastewater and industrial CO₂, and the mixture can be released into a raceway pond for the cultivation of marine algae and waste treatment. Algae not only help to remove nitrates, phosphates, and heavy metals from wastewater, but can also generate biomass and food (21, 22). Treated water from the waste module can then be released back into the environment. The cultivation of algae requires a set ratio of carbon molecules (C), nitrides (N), and phosphates (P); most algae species prefer a C:N:P ratio of 50:8:1, while typical municipal wastewater only has a C:N:P ratio of 20:8:1 (23). Thus, CO₂ can be dissolved in wastewater to increase the carbon percentage in order to maximize the efficiency of algae cultivation. The cultivation of algae has many other potentially useful applications aside from wastewater treatment, including the powering of power plants, the production of combustible gas through gasification of biomass, conversion of biomass into biofuels and hydrocarbon fuels, or fermentation, anaerobic digestion, and composting of biomass by microorganisms. In addition, many macroscopic species of algae are also frequently cultivated for human consumption.

In this research project, we inquired into the feasibility and efficiency of designing a facility for clean drinking water as a solution for current environmental issues including drought, greenhouse gases, and lack of sanitation. We propose a solar energy powered desalination plant primarily consisting of an energy module and a desalination module. To evaluate and optimize the components of our proposed model, we inquired into two specific issues, the trajectory and radiation energy of the sun over the course of a day, and the efficiency of various desalination methods. We constructed a solar tracking robot to track solar position and to harvest solar energy during the daytime, and we found that there was a linear increase in the azimuth angle and a parabolic change in the elevation angle of the sun, and that solar radiation was nearly constant during the daytime near the earth's surface in the test location. Cloud cover was found to be a major source of fluctuations in the data. We also conducted a series of small-scale simulation experiments to evaluate the efficiency of various desalination methods using the collected solar energy. According to our analysis, the most efficient desalination method is to harvest water vapor from sub-boiling saline water heated by solar energy. We demonstrated that each proposed desalination plant could provide fresh water for the domestic usage of approximately 25,000 people in California. Therefore, provided that such a plant is feasible, our proposed solution for renewable water and energy has the potential to revolutionize how the world

approaches sustainability issues.

Methods

In the first experiment, we constructed a robot using Lego components to track the position of the sun, as shown in Figure 2a. The light sensor module is mounted on a motor module that contains two motors, one rotating around the azimuthal axis and the other rotating around the elevation axis. A solar panel of area $6 \times 10 \text{ cm}^2$ was installed below and parallel to the sensor. At the base of the robot is a computer that controls the robot, along with an energy meter that was used to calculate energy input and output. The robot was controlled by a tracking algorithm (Figure 2b), that was programmed using the graphic-based Lego Mindstorms NXT programming software. The robot was programmed to rotate around the azimuth, the angular position of the sun relative to 0°N , as well as elevation, the angular position of the sun relative to the horizon, and comparing the brightness before and after the rotation to decide the next rotation. In doing so, it locates the brightest spot, the sun, in the sky and tracks its movement over the course of a single day.

The program commences the data logging function, after which it measures the ambient luminosity and rotates the robot $\pm 1^\circ$ azimuthally and elevation-wise. The control of azimuth and elevation run simultaneously on parallel loops. After each rotation, the algorithm makes another measurement of ambient luminosity and compares the luminosity to that before the rotation. If the luminosity has increased, the robot continues rotating in the same direction. Otherwise, if the luminosity has decreased, the robot rotates in the reverse direction. A copy of the tracking algorithm can be downloaded from <http://phy.ntnu.edu.tw/~cchen/pdf/tracking.rbt>.

In the first experiment, we aligned the robot to the north using a compass application. The solar tracking program was run from 9:45 A.M. to 2:45 P.M., collecting data concerning azimuth and elevation of solar position, as well as the current and voltage amplitudes generated by the solar panel. A cardboard tube was placed over the light sensor of the robot (Figure 2a) to allow the robot to focus on a smaller region of the sky and thus obtain more accurate results.

In the second experiment, saline water was desalinated by direct exposure to the sun (Figure 5a) and by heating with an induction cooker (Figure 5b). In the desalination experiment with direct exposure to the sun, we measured the amount of evaporated water from 1 L of saline water in a pan with an inner surface area approximately 0.1 m^2 . A thermometer was used to monitor the temperature of the saline water. The black inner surface of the pan was used in the experiment to absorb heat energy, while the silver outer surface reflected the majority of the heat energy. To compensate for the shadow cast by the pan, we mounted a mirror on the solar tracking robot to reflect sunlight to the inner surface of the pan. To collect water vapor, we placed a piece of plastic wrap on the top of the pan and secured it using a rubber band. A weight in the centre of the plastic

wrap caused it to sink, such that the vapor condensate would trickle down to middle of the plastic wrap and be collected by a small container below. The pan was placed in sunlight from 10 A.M. to 5 P.M., and the volume of the collected fresh drinking water was measured at the end of the trial.

As shown in Figure 5, we heated saline water in a pot using an induction cooker to simulate desalination in our hypothetical model. To simulate the removal of vapor out of the evaporation chamber by a pump, the pot was kept open to allow the diffusion of vapor. Saline solutions of 1%, 2%, 3%, 3.5%, and 5% salinity were prepared by respectively mixing 6 g, 12 g, 18 g, 21 g, and 30 g of salt with 600 mL of 15°C water in a large beaker. Each solution that we prepared, along with 600 mL of regular water as a control, was then heated in a pot that was placed on a 200 W induction cooker for 20 minutes. The size of the pot was also varied by using three different pots with respective diameters of 16 cm, 20 cm, and 23 cm. Over the course of the experiment, the temperature of saline water was kept below the boiling point, by monitoring a thermometer in the saline water. After heating, we used a smaller beaker to accurately measure the volume of the remaining saline water. Three trials were conducted for each combination of salinity and pot diameter, thus enabling more accurate and comprehensive calculations of averaged data.

Acknowledgments

RHGC thanks D. Coopersmith for the stimulating discussions and sources of inspiration at the University Transition Program of UBC.

References

1. Checchi F., and W. C. Robinson. "Mortality among populations of southern and central Somalia affected by severe food insecurity and famine during 2010-2012." Food Security and Nutrition Analysis Unit – Somalia, 2013. Print.
2. Lewis S.L., P.M. Brando, O.L. Philips, G.M.F. van der Heijden, and D. Nepstad. "The 2010 Amazon Drought." *Science* 331.6017 (2011): 554. Print.
3. Dai, A. "Drought under global warming: a review." *Wiley Interdisciplinary Reviews: Climate Change*. 2.1 (2011): 45-65. Print.
4. Blasing, T. J., and K. Smith. "Recent greenhouse gas concentrations." Updated July (2006). Web. 16 Aug. 2014.
5. Van der Werf, G.R., D.C. Morton, R.S. DeFries, J.G.J. Olivier, P.S. Kasibhatla, R.B. Jackson, G.J. Collatz, and J.T. Randerson. "CO₂ emissions from forest loss." *Nature Geoscience*. 2.11 (2009): 737-738. Print.
6. Henze, M. "Wastewater Characterization." *Biological Wastewater Treatment: Principles Modelling and Design*. Ed. M. Henze, M.C.M. van Loosdrecht, G.A. Ekama, and D. Brdjanovic. London: IWA Publishing, 2008. 33-52. Print.
7. Christophe, Bosch. "Project Information Document, Concept Stage: Delhi Water Supply & Sewerage." World Bank, 2006. Print.

8. Ebenstein, A.Y. "Water Pollution and Digestive Cancers in China." China Economics Summer Institute, 2008. Print.
9. Price, H., E. Lüpfer, D. Kearney, E. Zarza, G. Cohen, R. Gee and R. Mahoney. "Advances in Parabolic Trough Solar Power Technology." *Journal of Solar Energy Engineering*. 124.2 (2002): 109-125. Print.
10. Xu, Q., M. Cai, and Y. Shi. "Dynamic heat transfer model for temperature drop analysis and heat exchange system design of the air-powered engine system." *Energy*. 68 (2014): 877-885. Print
11. "Calculation of sun position in the sky for each location on the earth at any time of day." SunEarthTools.com. 16 Aug. 2014. Web. 16 Aug. 2014.
12. Jean Meeus, *Astronomical Algorithms* (Richmond: Willmann-Bell, 2005). Print.
13. Richards, J.M. "A simple expression for the saturation vapor pressure of water in the range -50 to 140 °C." *Journal of Physics D: Applied Physics*. 4.4 (1971): L15-L18. Print.
14. Loster, M. "Total primary energy supply from sunlight." Department of Physics. University of California 3, 2006. Print.
15. Bishop, J.K.B. and W.B. Rossow. "Spatial and temporal variability of global surface solar irradiance." *Journal of Geophysical Research: Oceans*. 96.C9 (1991): 16839-58. Print.
16. Barnett, C. "World groundwater recharge rate." *Ensis.com*. 19 Aug. 2013. Web. 16 Aug. 2014.
17. "Groundwater resources of the world." BGR & UNESCO. 2008. Web. 16 Aug. 2014.
18. Kenny, J.F., N.L. Barber, S.S. Hutson, K.S. Linsey, J.K. Lovelace, and M.A. Maupin. "Estimated Use of Water in the United States in 2005." U.S. Geological Survey. 11 Jan. 2013. Web. 16 Aug. 2014.
19. U.S. Census Bureau. *State & County Quickfacts: California, 2013*. Print.
20. U.S. Census Bureau. *State & County Quickfacts: Los Angeles, California, 2013*. Print.
21. Abdel-Raouf, N., A.A. Al-Homaidan, and I.B.M. Ibraheem. "Microalgae and wastewater treatment." *Saudi Journal of Biological Sciences*. 19.3 (2012): 257-75. Print.
22. Christenson, L. and R. Sims. "Production and harvesting of microalgae for wastewater treatment, biofuels, and bioproducts." *Biotechnology Advances*. 29 (2011): 686-702. Print.
23. Woertz, I., L. Fulton, and T. Lundquist. "Nutrient Removal & Greenhouse Gas Abatement with CO₂ Supplemented Algal High Rate Ponds." The WEFTEC annual conference, Water Environment Federation, October 12-14, 2009, Orlando, Florida. 13. Print.